Physics Letters B 845 (2023) 138149

Contents lists available at ScienceDirect

Physics Letters B

journal homepage: www.elsevier.com/locate/physletb

Cross-shell states in ^{15}C: A test for p-sd interactions

J. Lois-Fuentes [a], B. Fernández-Domínguez [a,*], X. Pereira-López [a,b,c], F. Delaunay [b], W.N. Catford [d], A. Matta [d,b], N.A. Orr [b], T. Duguet [e,f], T. Otsuka [g], V. Somà [e], O. Sorlin [h], T. Suzuki [i,j], N.L. Achouri [b], M. Assié [k], S. Bailey [l], B. Bastin [h], Y. Blumenfeld [k], R. Borcea [o], M. Caamaño [a], L. Caceres [h], E. Clément [h], A. Corsi [e], N. Curtis [l], Q. Deshayes [b], F. Farget [h], M. Fisichella [m], G. de France [h], S. Franchoo [k], M. Freer [l], J. Gibelin [b], A. Gillibert [e], G.F. Grinyer [n], F. Hammache [k], O. Kamalou [h], A. Knapton [d], Tz. Kokalova [l], V. Lapoux [e], B. Le Crom [k], S. Leblond [b], F.M. Marqués [b], P. Morfouace [k], J. Pancin [h], L. Perrot [k], J. Piot [h], E. Pollacco [e], D. Ramos [a], D. Regueira-Castro [a], C. Rodríguez-Tajes [a,h], T. Roger [h], F. Rotaru [o], M. Sénoville [b], N. de Séréville [k], R. Smith [l,1], M. Stanoiu [o], I. Stefan [k], C. Stodel [h], D. Suzuki [k], J.C. Thomas [h], N. Timofeyuk [d], M. Vandebrouck [h,e], J. Walshe [l], C. Wheldon [l]

[a] IGFAE and Dpt. de Física de Partículas, Univ. of Santiago de Compostela, E-15758, Santiago de Compostela, Spain
[b] LPC Caen UMR6534, Université de Caen Normandie, ENSICAEN, CNRS/IN2P3, F-14000 Caen, France
[c] Center for Exotic Nuclear Studies, Institute for Basic Science (IBS), Daejeon 34126, Republic of Korea
[d] Department of Physics, University of Surrey, Guildford GU2 5XH, UK
[e] IRFU, CEA, Université Paris-Saclay, F-91191 Gif-sur-Yvette, France
[f] KU Leuven, Instituut voor Kern- en Stralingsfysica, 3001 Leuven, Belgium
[g] CNS, University of Tokyo, 7-3-1 Hongo, Bunkyo-ku, Tokyo, Japan
[h] GANIL, CEA/DRF-CNRS/IN2P3, Bd. Henri Becquerel, BP 55027, F-14076 Caen, France
[i] Department of Physics, College of Humanities and Sciences, Nihon University, Sakurajosui 3-25-40, Setagaya-ku, Tokyo, Japan
[j] NAT Research Center, NAT Corporation, 3129-45 Hibara Muramatsu, Tokai-mura, Naka-gun, Ibaraki, 319-1112, Japan
[k] Université Paris-Saclay, CNRS/IN2P3, IJCLab, 91405 Orsay, France
[l] School of Physics and Astronomy, University of Birmingham, Birmingham B15 2TT, UK
[m] INFN, Laboratori Nazionali del Sud, Via S. Sofia 44, Catania, Italy
[n] Department of Physics, University of Regina, Regina, SK S4S 0A2, Canada
[o] IFIN-HH, P. O. Box MG-6, 76900 Bucharest-Magurele, Romania

ARTICLE INFO

Article history:
Received 14 February 2023
Received in revised form 2 August 2023
Accepted 22 August 2023
Available online 28 August 2023
Editor: Betram Blank

Keywords:
One neutron pick-up reaction
Neutron-rich carbon isotopes
Phenomenological shell-model
Ab initio calculations

ABSTRACT

The low-lying structure of ^{15}C has been investigated via the neutron-removal ^{16}C(d,t) reaction. Along with the known bound neutron sd-shell states, unbound p-shell hole states have been observed. The excitation energies and the deduced spectroscopic factors of the cross-shell states are an important measure of the $[(p)^{-1}(sd)^2]$ neutron configurations in ^{15}C. Our results show a very good agreement with shell-model calculations using the SFO-tls interaction for ^{15}C. However, this same interaction predicted energies that were too low for the corresponding hole states in the $N = 9$ isotone ^{17}O and adjustment of the *p-sd* and *sd-sd* monopole terms was required to match the ^{17}O energies. In addition, the excitation energies and spectroscopic factors have been compared to the first calculations of ^{15}C with the *ab initio* self-consistent Green's function method employing the NNLO$_{sat}$ interaction. The results show the sensitivity to the size of the $N = 8$ shell gap and highlight the need to go beyond the current truncation scheme.

1. Introduction

The shell structure of nuclei is one of the cornerstones of nuclear physics. The evolution of the shell structure observed in exotic nuclei has led to a change of paradigm in our understanding of the nuclear interaction [1]. Nuclei far from the stability with

* Corresponding author.
E-mail address: beatriz.fernandez.dominguez@usc.es (B. Fernández-Domínguez).
[1] Present address: Department of Engineering and Mathematics, Sheffield Hallam University, Howard Street, Sheffield, S1 1WB, United Kingdom.

https://doi.org/10.1016/j.physletb.2023.138149

large values of isospin are very sensitive to new aspects of nuclear forces.

In particular, the neutron-rich carbon isotopes have drawn much attention due to their properties: neutron halos [2,3], clustering [4], and deformation [5]. Such light neutron-rich systems offer an ideal testing ground for theoretical models. On the one hand, phenomenological shell-model calculations in the *p-sd* space with improved interactions, such as SFO-tls [6,7] or YSOX [8] have been very successful in describing the structure of neutron-rich carbon isotopes [9]. However, they fail at reproducing the energy levels of unnatural parity states across a given isotonic chain partly because of the lack of experimental data for cross-shell states in exotic nuclei. On the other hand, new interactions derived from chiral effective field theory [10,11] and rooted in quantum chromodynamics have made significant progress in the description of light and medium-mass nuclei [12,13]. The low-lying spectroscopy of ^{15}C obtained from the (d,t) reaction is an ideal observable to constrain not only phenomenological interactions but also nucleon-nucleon, NN, and three-body forces, $3NF$, derived from chiral effective field theory. Indeed, excitation energies and spectroscopic factors determined from single-particle transfer reactions provide one of the most stringent tests to *ab initio* wavefunctions derived from realistic nuclear forces.

We report here on the first investigation of the cross-shell states in ^{15}C using the ^{16}C(d,t) single-neutron pick-up reaction. Assuming a normal ordering in ^{16}C, protons occupy the *p*-shell and neutrons the *p-sd*-shell. With ^{14}C as a core, removing a neutron from the ^{16}C ground state will probe states with $(1p-0h)$ configurations in ^{15}C. Additionally, extracting a neutron from the $0p_{1/2}$ or $0p_{3/2}$ orbitals will give rise to states with two particle-one hole $(2p-1h)$ configurations across the $0p_{1/2}$ and $1s_{1/2}$-$0d_{5/2}$ orbits. States with spin and parity of $1/2^-$ and $3/2^-$ and large single-particle component are signatures of particle-hole excitations and can provide information on the amplitude of the $N=8$ shell gap.

Previous knowledge on the structure of ^{15}C has been gathered over the past decades using a variety of experimental probes: single-neutron adding reactions ^{14}C(d,p) [14–18], two-neutron transfer - ^{13}C(t,p) [19] and ^{13}C$(^{18}$O,^{16}O$)^{15}$C [20] - Coulomb breakup [21], β-delayed neutron decay of spin-polarized ^{15}B [22] and single-neutron knockout reactions from ^{16}C [23–25]. All these probes have provided extensive information, mainly on positive-parity states. However little is known about the negative-parity states. In particular, no p-shell hole states from single-neutron removal reactions are clearly established. Such states would be key for testing the shell-model interactions for the $p-sd$ model space, and potentially improving the description of other light exotic nuclei.

2. Experimental details

The experiment was performed at GANIL using a secondary ^{16}C beam produced by fragmentation in the LISE spectrometer at 17.2 MeV/nucleon with an intensity of $\sim 5\times10^4$ pps and 100% purity. The target consisted of a CD_2 foil of 1.37(4) mg/cm^2 thickness. A set of two multiwire proportional chambers [26] was used to track the beam onto the target on an event-by-event basis and served also as time reference and to measure the incoming beam intensity. The target was surrounded by the TIARA Silicon array [27] comprising an octagonal double-layered barrel of resistive strip detectors spanning 36° to 144° and an annular double-sided silicon strip detector covering the most backward angles (144° - 169°). This allowed data to be also acquired for the ^{16}C$(d,p)^{17}$C reaction, discussed elsewhere [28] and for the ^{16}C$(d,d)^{16}$C elastic scattering. Light-ejectiles emitted from the neutron removal reaction ^{16}C$(d,t)^{15}$C were detected by three MUST2 telescopes [29] placed in the forward hemisphere at 15 cm downstream the target

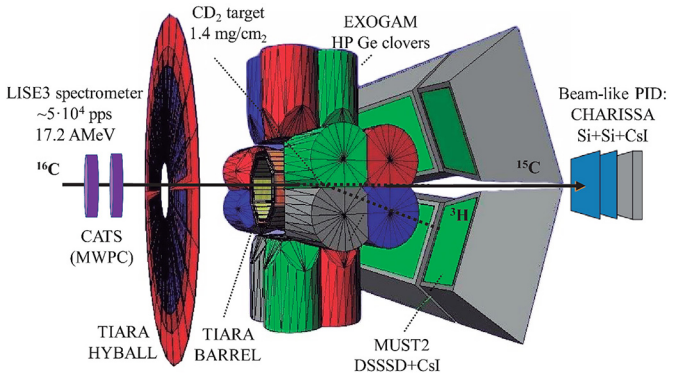

Fig. 1. Schematic view of the experimental set-up.

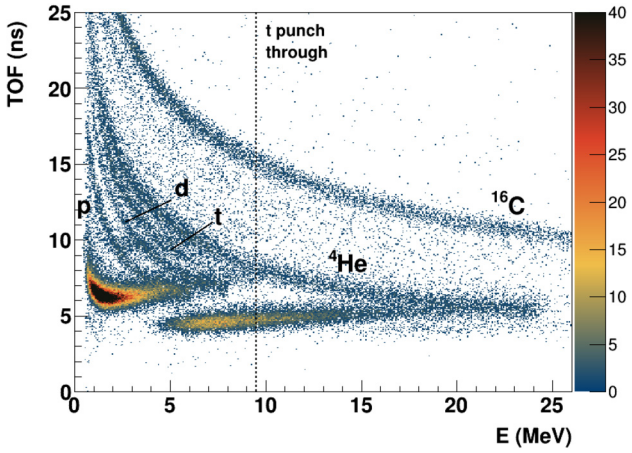

Fig. 2. Identification matrix: Time-Of-Flight (TOF) in ns between MUST2 and the first beam tracking detector versus the energy in MeV measured in the first layer of the MUST2 telescope. The dashed line shows the triton punch-through.

covering angles from 10° to 40° in the laboratory frame. The first layer of the MUST2 telescopes consisted of 300-μm thick double-sided silicon strip detectors (DSSSD) that provided measurements of the total energy, the angle and served as the start signal for the time of flight (TOF). The stop signal was obtained from the multiwire proportional chambers placed upstream of the target. The beam-like fragments were detected in a Si-Si-CsI telescope located at zero degrees 33 cm downstream of the target [30]. Only atomic-number identification of the beam-like fragments was achieved. Gamma-rays from the dexcitation of the recoil were measured in coincidence in the four germanium clover detectors of the EXOGAM array [31] placed at 90° surrounding the barrel at a distance of 55 mm from the centre of the target. The only bound excited state in ^{15}C is at 0.740 MeV with a half-life of 2.61 ns [32] similar to the flight time from the target to MUST2. Additionally, the unbound states measured in this work are below the threshold for decay to the first excited state in ^{14}C (6.09 MeV [32]) and therefore no γ-rays were observed in coincidence with the tritons. Other results from this experimental campaign have been published previously, and more details on the experimental set-up can be found in references [28,33,34]. A schematic view of the set-up is shown in Fig. 1.

Tritons from the (d,t) reaction, which stopped in the DSSSD, have been identified using the E-TOF technique, as shown in Fig. 2. Atomic mass information can be obtained from the following expression, knowing the flight path of each particle from the target to the telescope:

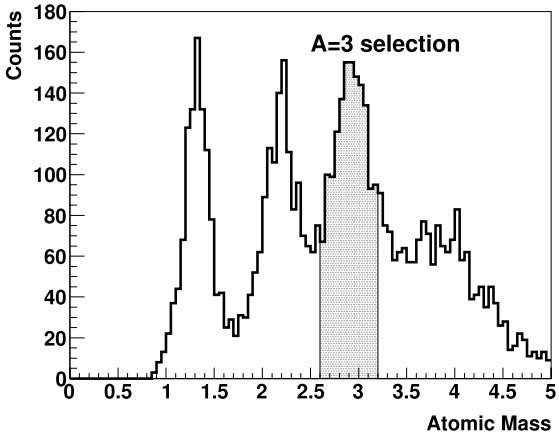

Fig. 3. Mass spectrum for the light ejectiles measured in MUST2. The A=3 selection was taken for events between 2.6 and 3.2.

$$A = \frac{2E}{u}\left(\frac{TOF}{L}\right)^2 \quad (1)$$

where E is the kinetic energy, u the atomic mass unit, L the flight path obtained from the positions of the particle in MUST2 and of the beam ion on target. Fig. 3 shows the mass identification for particles with total kinetic energy E < 8 MeV. Note that the mass calibration was for tritons and therefore the other peaks are slightly shifted. While only mass-separation is possible with this method, contamination from ^{3}He particles is not expected below 8 MeV owing to the kinematics of the ^{16}C$(d,^3He)$ reaction.

The dependence of the resolution with excitation energy was determined using the *Nptool* simulation package [35]. The simulation included the straggling of the particles in the different material layers of the detectors and in the target, the geometry of the setup, the resolution of the different detectors and the secondary beam energy spread and the reconstructed beam spot size.

3. Results

The (d,t) events were selected as coincidences of an A=3 particle with energy below 8 MeV and a Z=6 heavy residue in the zero-degree telescope. Excitation energy from the single-neutron pickup channel was reconstructed using the missing-mass technique and the resulting spectrum in the center-of mass angular range between 3°-15° is displayed in Fig. 4. From the (d,t) data, three clear peaks are observed in Fig. 4. Due to the low-energy of the tritons ($Q_0 = 2.0$ MeV) and their energy-loss straggling in the target, the resolution in excitation energy is not sufficient to separate the individual contributions below the neutron-separation threshold ($S_n = 1.218$ MeV). In fact, the broad peak around 0 MeV corresponds to the $1/2^+$ ground state and the $5/2^+$ isomeric state at 0.74 MeV of ^{15}C [32]. The bound states were represented, based on the detailed simulations, by asymmetric lineshapes that accounted for the experimental effects (most notably the effects of straggling). Voigt functions were employed for the unbound states. Additionally, the contributions from a three-body final state (^{14}C+n+t) together with the background from masses with A=2 and 4 were included in the fit (Fig. 4). The three-body contribution was obtained by uniformly sampling the phase-space of such a decay.

From the (d,t) data, four states are observed in ^{15}C: the ground state, the 0.74 MeV isomeric state and two states at 2.76(31) and 5.41(32) MeV.

The resonance at 2.76 MeV was already observed in the ^{14}C$(d,p)^{15}$C [16], ^{13}C$(t,p)^{15}$C [19] and ^{13}C$(^{18}$O,^{16}O$)^{15}$C [20] experiments at approximately 3.10 MeV and assigned a spin and

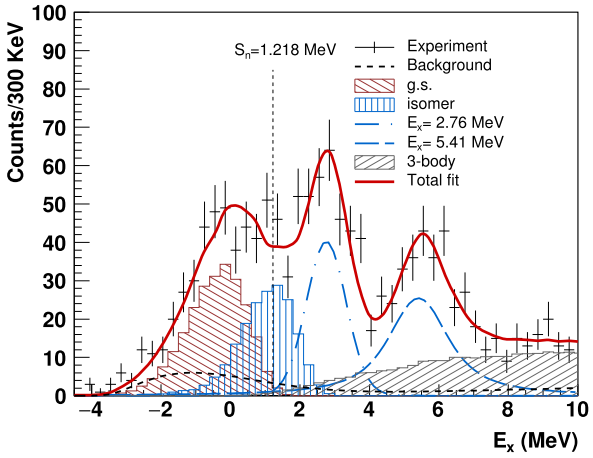

Fig. 4. Experimental excitation energy spectrum for ^{15}C obtained in the reaction ^{16}C$(d,t)^{15}$C for the angular range 3°-15° in the center of mass. Bound states are represented by histograms obtained from simulations (see text) while dash-dotted curves correspond to the unbound states. The light grey filled histogram shows the contribution from the three-body final state (^{14}C+n+t) and the dashed line that from the background from neighbouring masses. The solid-red curve is the total fit to the spectrum.

parity of $1/2^-$. For the 5.41 MeV resonance, several states have been observed around this region but no definitive assignments have yet been made. As noted earlier, the tritons over the angular range measured here had very low-energies ($\sim$ 1.0-2.5 MeV). As such, the energy loss and straggling in the target and possible non-linearities in the MUST2 array's response (notably the ADCs) resulted in uncertainties in the determination of the energies and the reconstructed excitation energies. As may be seen in Table 1, deviations of around 300 keV were found between the values deduced here with respect to the known excitation energies and a systematic uncertainty of this size has been included in the final uncertainties.

Differential cross-sections for 3-4 angular-bins of 2° width have been reconstructed. The angular range was limited, from 3°-15° in the center of mass, in order to avoid abrupt changes in acceptance. The angular distributions are shown in Fig. 5, and are compared to finite-range, prior form Distorted-Wave Born Approximation (DWBA) calculations using the code FRESCO [36]. For the d+^{16}C entrance channel, the optical model parameters were obtained from the global parameterisation of Haixia et al. [37], modified to reproduce d+^{16}C elastic scattering measured here at the same time as ^{16}C(d,t) [34]. The elastic data showed that an increased diffuseness of the imaginary part of the optical potential was needed [34]. For the t+^{15}C exit channel the optical model potential from Pang et al. [38], was employed. The $\langle d|t\rangle$ overlap was computed in a potential reproducing results from Green's function Monte Carlo calculations [39]. The $\langle^{16}$C$|^{15}$C$\rangle$ overlaps were represented by bound neutron wave functions obtained in a Woods-Saxon potential with standard geometry (radius parameter $r_0 = 1.25$ fm and diffuseness $a = 0.65$ fm), and with the depth adjusted to reproduce the effective neutron separation energy.

From the shape of the angular distributions the orbital angular momentum of the removed nucleon for the ground and isomeric states were found, as discussed below, to reproduce the known values. Additional arguments were also employed for the unbound levels. Spectroscopic factors were deduced initially by normalising the calculated angular distributions to the data. In order to explore the sensitivity of the results to the choice of the optical model potentials, combinations of five different entrance channel [28,37,40–42] and two different outgoing channel potentials [38,43] were explored. The spectroscopic factors deduced in this fashion varied significantly, with $C^2S(1s_{1/2})$= 0.28-0.35 for

Table 1
Spin-parity assignments J^π, excitation energies E_x (keV), normalised spectroscopic factors C^2S, asymptotic normalization coefficients squared (C_n^2) and corresponding transferred angular momenta ℓ for the states observed in ^{15}C, compared to previous experimental data and shell model predictions with the SFO-tls interaction and to results of SCGF calculations using the NNLO$_{sat}$ interaction. The quoted uncertainties include statistical and fitting errors, systematic uncertainties arising from the reaction modelling (20%) and the error in the target thickness (3%).

E_x (keV)	E_x (keV)[a]	ℓ	J^π	C^2S[c]	C_n^2 (fm^{-1})	J^π	E_x (keV)	C^2S	E_x (keV)	C^2S
(d,p)			(d,t)				SFO-tls		NNLO$_{sat}$	
[32]			(present)							
0	0.00(36)[b]	0	$1/2^+$	0.65(16)	8.66(17)	$1/2^+$	0.0	0.64	0.168	0.51
0.740 (1)	1.10(37)	2	$5/2^+$	1.35(32)	1.56(3)	$5/2^+$	0.854	1.20	0.00	1.10
3.103 (4)	2.76(31)	1	$1/2^-$	1.74(23)	14.23(31)	$1/2^-$	2.74	1.35	6.62	0.35
						$1/2^-$	4.71	0.10	7.88	1.11
	5.41(32)	1	$3/2^-$	1.25(24)	24.38(54)	$3/2^-$	5.30	0.62	10.63	0.63
						$3/2^-$	6.00	0.68	10.80	1.14

[a] The uncertainty includes a contribution of 0.3 MeV arising from the determination of the triton energies.
[b] The ground state energy was set to zero although the measured value differs within the quoted uncertainty (see text).
[c] Normalised (see text) such that summed C^2S for the $1/2^+$ and $5/2^+$ levels is 2.0.

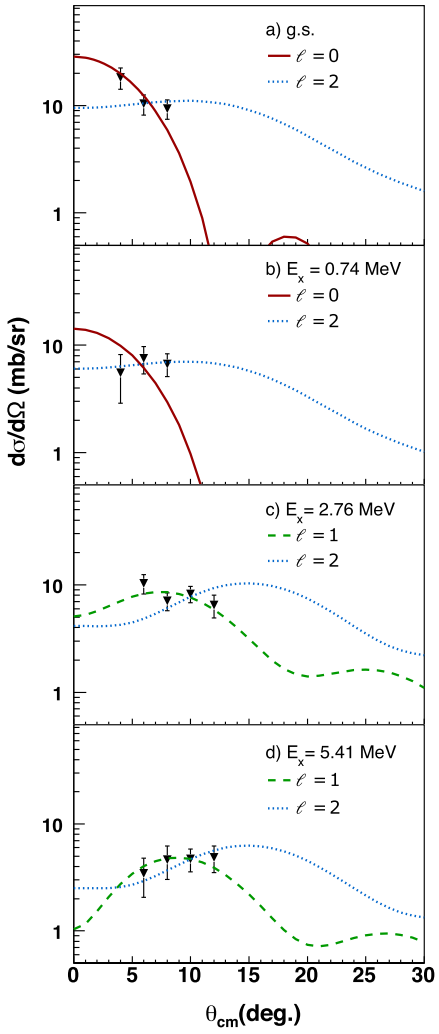

Fig. 5. Angular distributions for the ground state (a) the first excited state (b) and the two observed resonances in ^{15}C at 2.76 (c) and 5.41 (d) MeV compared to $\ell =$ 0, 1, 2 (red, green, and blue) DWBA calculations. The uncertainties in the angular distributions are statistical. The displayed cross-sections are not normalized to the occupancy of the *sd*-shell.

the ground state and $C^2S(0d_{5/2})$=0.35-0.56 for the isomeric level. Importantly the shapes of the angular distributions did not vary in any appreciable manner for any of the states (bound and unbound) over the angular range measured.[2] Moreover, the relative spectroscopic strengths between the states also did not change appreciably with the choice of optical potentials and rather it was the absolute normalisation that varied. Given the broad range of normalisations for the spectroscopic factors, according to the potentials employed, the sum of the spectroscopic factors for the $1/2^+$ ground and $5/2^+$ isomeric state have been set to be 2 [1]. This assumes ^{16}C to have precisely two neutrons in the *sd*-shell outside a ^{14}C core. The assumption of a ^{14}C core is supported by measurements of the $(d,^3He)$ reaction on carbon isotopes [44] which indicate that the number of protons in the $\pi 0p_{1/2}$ orbital is lower in ^{14}C compared to ^{12}C owing to the presence of neutrons in the $0p_{1/2}$ orbital. In addition, the sum of the spectroscopic factors for the ground and first excited state in ^{15}C has been found to be close to unity in a study of the ^{14}C (d,p) reaction [18]. It may also be noted that the $1/2^+$ and $5/2^+$ states in ^{13}C are only weakly populated in the ^{14}C (p,d) reaction [14,45]. The normalisation of the summed strength of the $1/2^+$ ground and $5/2^+$ states to be 2, as adopted here, disregards the occupancy of the $0d_{3/2}$ orbital. However, this contribution is expected to be no more than 10% (see, for example, the shell model calculations discussed below) – a contribution much smaller than the experimental uncertainties. Importantly, the normalisation employed for the $1/2^+$ and $5/2^+$ states is also applied to the unbound states.

The top panel of Fig. 5 shows the $\ell = 0$ character of the angular distribution for the ground state (see Fig. 5 (a)) which is consistent with the known assignment of $1/2^+$ [18,24,25]. The angular distribution for the peak at approximately 0.74 MeV (see Fig. 5 (b)) displays an $\ell = 2$ contribution in agreement with the $5/2^+$ assignment by Refs. [18,24,25].

Fig. 5 (c) shows the angular distribution for the first resonance at 2.76(31) MeV. The $\ell = 2$ curve yields an unphysical occupancy of the state. The available strength of the $0d_{5/2}$ orbital for the single-neutron pick-up is almost exhausted by the isomeric state at 0.74 MeV as the remaining strength has been observed in the ^{16}C$(d,p)^{17}$C reaction [28]. Based on the Macfarlane-French sum rule for C^2S [46], where the occupancy is $G^-(0d_{5/2}) = 1.35(32)$ (see Table 1) and the vacancy is $G^+(0d_{5/2}) = \frac{2J_f+1}{2J_i+1}\ C^2S = 6 \times 0.62(13)$ ([28]), the observed single-particle strength adds up to 84.5(75)% of the total. In addition, the $\ell = 1$ transfer is favoured by the data. Therefore, the spin and parity of the 2.76(31) MeV is inferred to be $1/2^-$ in agreement with earlier studies [16,19,20]. The

[2] It is possible that data of higher statistical quality covering a much wider range of angles may allow the most suitable optical model potentials to be determined.

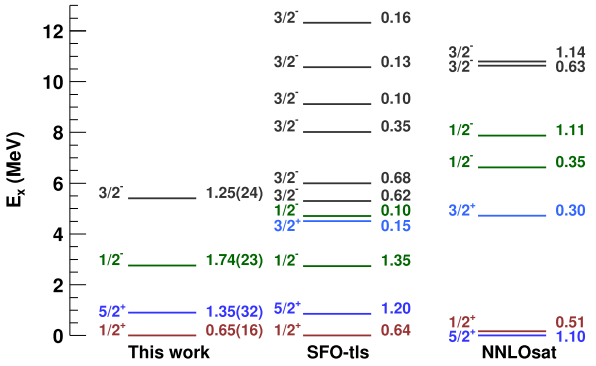

Fig. 6. Experimental level scheme for ^{15}C compared to the results of the shell model with the SFO-tls interaction and to SCGF calculations using the NNLO$_{sat}$ interaction. The column on the right represents the spectroscopic factor and on the left the spin and parity assignment.

configuration of this state thus corresponds to neutron removal from the $0p_{1/2}$ orbital in ^{16}C.

The angular distribution presented in Fig. 5 (d) corresponds to the state at 5.41(32) MeV. Only the comparison to the $\ell = 1$ calculation yields a reasonable spectroscopic factor, while that for $\ell = 2$ is incompatible with an acceptable occupation of the $0d_{5/2}$ or $0d_{3/2}$ orbitals in the ground state of ^{16}C. In addition, assuming a $1/2^-$ assignment for this state, the summed C^2S would greatly exceed the maximum number of neutrons allowed in the $0p_{1/2}$ orbital. Given the large spectroscopic factor and guided by the structure calculations presented in Table 1, we assign this state to be a neutron $0p_{3/2}$ hole and, therefore, a spin and parity of $3/2^-$. Previous results in references [19,20] and [22] point to a state at 5.88 MeV with a tentative $1/2^-$ assignment, although $3/2^-$ could not be totally excluded. Owing to the high excitation energy of the first excited state in ^{14}C, the resonance states populated here in ^{15}C can only decay by neutron emission to the ground state of ^{14}C.

Pick-up reactions such as (d, t) are of peripheral nature and represent a suitable tool to extract information on the asymptotic tail of the radial overlap function which is very sensitive to the *NN* interactions used in microscopic calculations [47]. The asymptotic normalization coefficient (ANC) squared C_n^2 was obtained as the product of the experimental spectroscopic factor S_{lj} and the square of the single-particle ANC b_{lj}. Spectroscopic factors extracted from peripheral reactions are usually sensitive to the choice of the neutron-nucleus potential used to generate the bound state wave function of the transferred nucleon [48,49]. In order to estimate this effect, the radius of the single-particle Woods-Saxon potential was varied from 1.15 to 1.35 fm and the resulting relative spectroscopic factors changed with respect to the standard value of 1.25 fm as follows: 35% ($0d_{5/2}$), 10% ($1s_{1/2}$), 20% ($0p_{1/2}$), 25% ($0p_{3/2}$) while the ANC remained constant within 1-3%, showing the peripheral character of the reaction. Therefore, in addition to the spectroscopic factors, the ANCs for the four states populated in ^{15}C are also reported in this work (see Table 1).

4. Discussion

The results are displayed in Table 1 and in Fig. 6 where the experimental level scheme is compared to state-of-the art shell-model calculations using the SFO-tls interaction [6,7] within the *p-sd* model space. This interaction has proven to be successful in reproducing the level ordering and single-neutron spectroscopic factors [28] as well as the magnetic dipole transitions in ^{17}C [7]. Additionally, we compare our results with *ab initio* many-body calculations using the self-consistent Green's function (SCGF) method at second order [50,51] with the NNLO$_{sat}$ interaction [12] from chiral effective field theory. The two-nucleon and three-nucleon forces were optimised to reproduce low-energy experimental observables in order to provide improved predictions for mid-mass nuclei [12]. In particular, the *NN*+3*NF* fit at next-to-next-to-leading order includes, apart from the nucleon-nucleon scattering data, the binding energies of ^{3}H, ^{3,4}He, ^{14}C, and ^{16,22,24,25}O together with the charge radii of the first five isotopes. The resulting interaction NNLO$_{sat}$ improves significantly the properties of mid-mass nuclei and reproduces the saturation point of nuclear matter [12,13,52,53] but has seldom been tested for the spectroscopy of $p - sd$ shell nuclei.

Positive-parity states in ^{15}C measure the one-particle zero-hole configurations ($1p - 0h$). The ratio of the $0d_{5/2}$ strength with respect to the $1s_{1/2}$ obtained in this work is in good agreement with the results from [23–25] within the error bars. Both states are well reproduced by the shell model with the SFO-tls interaction taking into account the experimental uncertainties. As for the SCGF calculations employing the NNLO$_{sat}$ interaction, the $1/2^+$ and $5/2+$ states are almost degenerate in energy, and the spectroscopic factors are in line with the experimental results.

The deduced ^{15}C spectroscopic factors can be compared to those obtained for the isotone ^{17}O in the ^{18}O(d, t) reaction by G. Mairle et al., [54] where the spectroscopic factors for the $C^2S(0d_{5/2})$ and $C^2S(1s_{1/2})$ are 1.53 and 0.21, respectively. The rise in the $0d_{5/2}$ spectroscopic strength in ^{17}O, as protons are added to the $0p_{1/2}$ orbital, shows an increase in the filling of the $0d_{5/2}$ orbital, due to the inversion of the $0d_{5/2}$ and $1s_{1/2}$ single-particle orbitals as described in reference [1]. Nevertheless, the filling of the $0d_{5/2}$ orbital in ^{16}C remains dominant due to pairing effects.

Above the neutron separation threshold in ^{15}C, negative-parity states appear with a $2p - 1h$ structure. As shown by the experimental spectroscopic factor (Table 1), the $1/2^-$ state contains a significant fraction of the total $0p_{1/2}$ strength. In fact, the observed strength for this state represents 87% of the total occupancy assuming an independent particle filling. The configuration of this state is interpreted to be a ^{13}C (g.s.)$\otimes(1s_{1/2}0d_{5/2})^2$ configuration in view of the large $(\nu 0p_{1/2})^{-1}$ spectroscopic factor. The excitation energy of the $1/2^-$ state provides some qualitative information on the size of the N=8 gap. While the shell model with the SFO-tls interaction reproduces the energy of the state that carries the main fragment of the $\nu 0p_{1/2}$ strength, the SCGF with NNLO$_{sat}$ calculation places this state at much higher energy (Fig. 6). This is mainly due to the lack of $(2p - 1h)$ configurations in the latter's theoretical scheme, which is truncated at second order. Additionally, the NNLO$_{sat}$ interaction generates a large mean-field gap between the *p* and *sd* harmonic-oscillator shells, which further hinders relevant cross-shell correlations.

Turning to the $0p_{3/2}$ strength in ^{15}C, as shown in Fig. 6 the theoretical strength distributions are significantly fragmented, especially in the shell-model calculations with SFO-tls. The experimental strength for the $0p_{3/2}$ orbital is 1.25(24) compared to the independent single-particle expectation of 4, therefore indicative of a significant fragmentation, with a large fraction of the strength possibly at higher excitation energy. As shown in Fig. 6 there are several states predicted by shell model calculations above 8 MeV that could not be seen in our experiment due to the limited statistics and resolution. The experimental total strength thus represents a lower limit. The excitation energy of the strongest $3/2^-$ state is in good agreement with the results from the shell model, showing that the state we see might be a combination of the two resonances predicted in the region. This is supported by the measured width of the state $\Gamma = 1.98(33)$ MeV which greatly exceeds the expected width of $\Gamma^{\ell=1} = 100$ keV[3] at the observed energy. Sim-

[3] Determined from the single-particle width and the SFO-tls spectroscopic factor for the $\ell = 1$ decay of the first $3/2^-$ state.

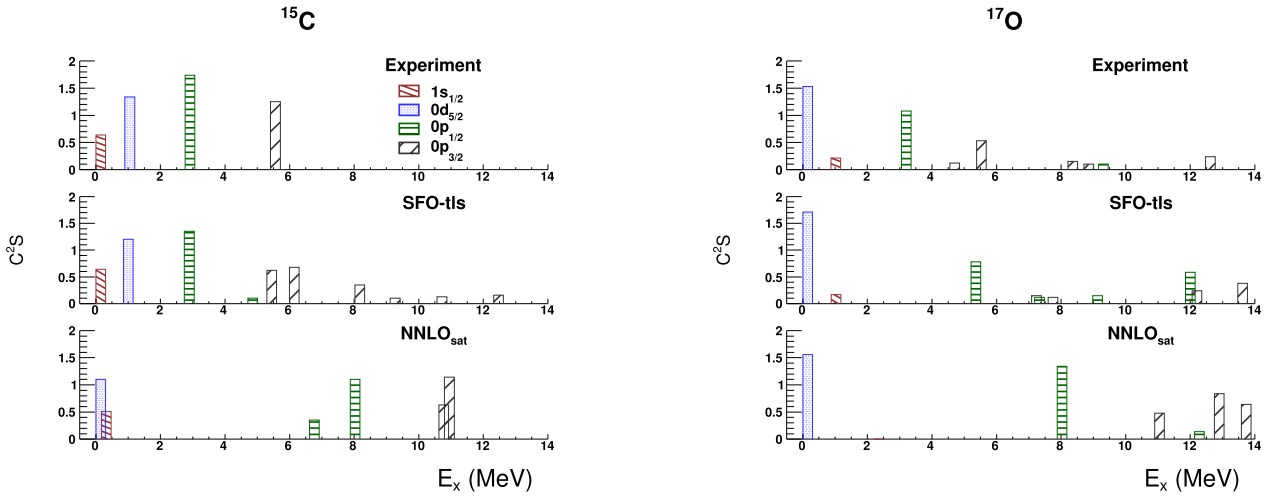

Fig. 7. Distribution of the measured single-particle strength C^2S for ^{15}C (left) and ^{17}O (right) as a function of excitation energy in MeV. Data from the ^{18}O$(d,t)^{17}$O reaction correspond to reference [54].

ilarly to what we observed for the $1/2^-$ state, the predictions for the $3/2^-$ state from the SCGF calculations with NNLO$_{sat}$ appear at much higher excitation energy. Surprisingly, the total strength is in reasonable agreement with the experimental results. It is important to note that the difference in energy between the major fragments of the $3/2^-$ and $1/2^-$ states is well reproduced ($\Delta_{N=6} \approx$ 2.9 MeV) which suggests that the mechanism at play, and the corresponding missing correlations in SCGF calculations, are indeed the same for the two states.

The $2p-1h$ configurations of the 2.76 and 5.41 MeV states are clearly established. As shown by the spectroscopic factors (Table 1), the $1/2^-$ and $3/2^-$ states contain a sizeable part of the total $0p_{1/2}$ and $0p_{3/2}$ strength $(sd)^2(0p)^{-1}$. Although part of the strength is expected at higher excitation energies, we can compare our results with those obtained in neutron removal from ^{18}O in the same excitation energy range.

Fig. 7 shows the measured strength from the (d,t) reaction as a function of the excitation energy for ^{15}C and ^{17}O. In the case of ^{15}C, there is a very good agreement between the experimental distribution of the single-particle strength and major fragments from the shell model using SFO-tls, with the exception of a higher degree of fragmentation in the shell-model $0p_{3/2}$ strength, not observed in our experiment, most possibly because of limited statistics and resolution. While the results of the SCGF calculations using the NNLO$_{sat}$ Hamiltonian agree well with experiment for the natural parity states, cross-shell states are, however overpredicted in energy.

Experimentally, the ordering of the $1/2^+$ and $5/2^+$ changes between ^{15}C and ^{17}O, which is indicative, as described in Ref. [1] of a significant modification in the $1s_{1/2}$ and $0d_{5/2}$ orbitals.

Owing to its single-particle character, the excitation energy of the $1/2^-$ state provides a measure of the N=8 shell gap. Experimentally, this state is observed at rather similar energies in both isotones - 2.76(31) MeV in ^{15}C and 3.055 MeV in ^{17}O pointing to a comparable N=8 shell gap. However, the single-particle strength of the $1/2^-$ state is more fragmented in ^{17}O as a consequence of an increase of correlations in the N=Z core (^{16}O). Theoretically, the SFO-tls interaction which gave a good account of the ^{15}C $2p-1h$ structure overestimates the size of the N=8 shell gap by some 1.5 MeV and also the position of the centroid for the $0p_{3/2}$ orbital appears to be shifted to higher energy by a similar amount. The large difference in energy for the negative-parity states in ^{17}O might be explained as a consequence of their configurations. The structure of the $1/2^-$ and $3/2^-$ states can be interpreted as ^{16}O$(3^-) \otimes 0d_{5/2}$ in the weak coupling model. In fact, experimentally the excitation energy of the first 3^- state in ^{16}O is found to be 6.13 MeV [32] while the SFO-tls interaction predicts it to at 7.633 MeV, which is 1.5 MeV higher than expected.

The shell model calculations using the SFO-tls interaction had to be modified in order to reproduce the ^{17}O level scheme. Valence particles are more weakly bound in the neutron-rich carbon isotopes compared with the oxygen isotopes. Note that the valence neutron in ^{15}C has a halo structure with one-neutron separation energy of 1.218 MeV. Effective nuclear forces that involve weakly bound neutrons are expected to be weaker than those for normal nuclei [55]. As the SFO-tls is constructed, in particular, to explain the structure of neutron-rich carbon isotopes, it is reasonable to use stronger nuclear forces in the oxygen isotopes. As such, monopole terms of two-body matrix elements that involve valence particles in the *sd*-shell are enhanced compared to the carbon case. The monopole terms of the $p-sd$ and $sd-sd$ matrix elements were made more attractive by 0.375 MeV in the isospin T=0 channel and by 0.125 MeV in the isospin T=1 channels than the original SFO-tls. The calculated distribution of the strength with the modified SFO-tls interaction (SFO-tls-mod) is found to be consistent with the experimental data. The effect of this modification is a lowering in the energy of the negative-parity states by approximately 1.5 MeV (SFO-tls-mod results are not shown in Fig. 7). The values obtained for the N=8 shell gap in the calculations are 9.05 MeV in ^{15}C (SFO-tls) and 8.33 MeV in ^{17}O (SFO-tls-mod) pointing to a rather constant value as observed experimentally.

Concerning the $3/2^-$ state, the major fragment of the strength appears at excitation energies around $\sim$ 5.5 MeV in the experimental spectra of ^{15}C and ^{17}O. The distribution of the strength for the $3/2^-$ states predicted theoretically by shell model calculations using the SFO-tls and SFO-tls-mod interactions seem to split the occupancy between two closely spaced states. As for the N=6 gap, it is difficult to draw any conclusions considering that only about 1/3 of the total strength has been observed in our experiment and it appears to be fragmented over several states.

Regarding the results of ^{17}O obtained from the SCGF calculations with NNLO$_{sat}$, we observe a similar behaviour as in ^{15}C - that is, an overestimation of the N=8 gap whereas N=6 is fairly well reproduced, suggesting a general trend from Z=6 to 8. Moreover, when going from ^{17}O to ^{15}C, the increase in fragmentation of the $5/2^+$ state and the associated population of the $1/2^+$ state are also well described. Conversely, the phenomenological SFO-tls interaction works locally in the region of Z=6 but further modifications in the monopole terms are needed when applying the same Hamiltonian to other regions of the $p-sd$ shell.

5. Summary

In summary, the results of the ^{16}C$(d,t)^{15}$C reaction presented here provide new information on the *p-sd* orbitals in ^{15}C. The results obtained for the positive parity states are in line with the established inversion of the neutron $1s_{1/2}$ and $0d_{5/2}$ single-particle orbitals. The variation in the relative strength of the single-particle orbits $1s_{1/2}$ and $0d_{5/2}$ along the N=9 isotonic chain, from ^{15}C to ^{17}O, results from the combined effects of the shell evolution mechanism due to the monopole interaction [1] and pairing.

The relative position of the $1/2^-$ and $3/2^-$ levels, with respect to the positive-parity states, is sensitive to the size of the N=8 shell gap. Calculations using the SFO-tls interaction agree well with the results obtained here for ^{15}C. However, the comparison with its isotone ^{17}O (N=9), showed the need to modify the monopole terms of the *p-sd* and *sd-sd* two-body matrix elements by 0.375 MeV in the T=0 channel and by 0.125 MeV in the T=1 channel.

While *ab initio* SCGF calculations reproduce the fragmentation of positive-parity states in ^{15}C, negative-parity states appear too high in energy. This highlights an increased N=8 shell gap and missing $2p-1h$ correlations in the current approximations and provides a strong motivation for extending the approach to higher orders [56].

Declaration of competing interest

The authors declare that they have no known competing financial interests or personal relationships that could have appeared to influence the work reported in this paper.

Data availability

Data will be made available on request.

Acknowledgements

J.L.F. wishes to acknowledge financial support from Xunta de Galicia (Spain) grant number ED481A-2020/069, X.P.L. acknowledges support through an IN2P3/CNRS (France) doctoral fellowship, the ST/P003885 grant (Spain) and Grant No. IBS-R031-D1. This work was supported by the Spanish MINECO through the project PGC2018-096717-B-C22 and PID2021-128487NB-I00. This work was also partially supported by the Xunta de Galicia under project No ED431B 2018/015, 2021-PG045 and the Maria de Maeztu Unit of Excellence MDM-2016-0692. W.N.C., N.T. and A.M. acknowledge financial support from the STFC grant number ST/L005743/1. M.F., N.C., Tz.K. and C.W. acknowledge support from STFC grant number ST/V001043/1. The authors acknowledge the support provided by the technical staff of LPC-Caen and GANIL. SCGF calculations were performed by using HPC resources from GENCI-TGCC (Contract no. A0110513012). The participants from the Universities of Birmingham and Surrey, as well as the INFN and IFIN-HH laboratories also acknowledge partial support from the European Community within the FP6 contract EURONS RII3-CT-2004-06065.

References

[1] T. Otsuka, A. Gade, O. Sorlin, T. Suzuki, Y. Utsuno, Rev. Mod. Phys. 92 (2020) 015002.
[2] D. Bazin, et al., Phys. Rev. C 57 (1998) 2156.
[3] D.Q. Fang, et al., Phys. Rev. C 69 (2004) 034613.
[4] M. Freer, H. Horiuchi, Y. Kanada-En'yo, D. Lee, U.-G. Meißner, Rev. Mod. Phys. 90 (2018) 035004.
[5] I. Hamamoto, Phys. Rev. C 76 (2007) 054319.
[6] T. Suzuki, R. Fujimoto, T. Otsuka, Phys. Rev. C 67 (2003) 044302.
[7] T. Suzuki, T. Otsuka, Phys. Rev. C 78 (2008) 061301(R).
[8] C. Yuan, et al., Phys. Rev. C 85 (2012) 064324.
[9] S. Kim, et al., Phys. Lett. B 836 (2023) 137629.
[10] E. Epelbaum, H.-W. Hammer, U.-G. Meißner, Rev. Mod. Phys. 81 (2009) 1773.
[11] R. Machleidt, D.R. Entem, Phys. Rep. 503 (2011) 1.
[12] A. Ekström, et al., Phys. Rev. C 91 (2015) 051301(R).
[13] V. Somà, P. Navrátil, F. Raimondi, C. Barbieri, T. Duguet, Phys. Rev. C 101 (2020) 014318.
[14] F.E. Cecil, J.R. Shepard, R.E. Anderson, R.J. Peterson, P. Kaczkowski, Nucl. Phys. A 255 (1975) 243.
[15] J.D. Goss, et al., Phys. Rev. C 8 (1973) 514.
[16] J.D. Goss, et al., Phys. Rev. C 12 (1975) 1730.
[17] G. Murillo, S. Sen, S.E. Darden, Nucl. Phys. A 579 (1994) 125.
[18] B. Kay, et al., Phys. Rev. Lett. 579 (2022) 125.
[19] S. Truong, H.T. Fortune, Phys. Rev. C 28 (1983) 977.
[20] F. Cappuzzelo, et al., Phys. Lett. B 711 (2012) 347.
[21] U. Datta-Pramanik, et al., Phys. Lett. B 551 (2003) 63.
[22] H. Miyatake, et al., Phys. Rev. C 67 (2003) 014306.
[23] E. Sauvan, et al., Phys. Lett. B 491 (2000) 1.
[24] V. Maddalena, et al., Phys. Rev. C 63 (2001) 024613.
[25] T. Yamaguchi, et al., Nucl. Phys. A 724 (2003) 3.
[26] S. Ottini-Hustache, et al., Nucl. Instrum. Methods A 431 (1999) 476.
[27] M. Labiche, et al., Nucl. Instrum. Methods A 614 (2010) 439.
[28] X. Pereira-López, et al., Phys. Lett. B 811 (2020) 135939.
[29] E. Pollacco, et al., Eur. Phys. J. A 25 (2005) 287.
[30] N.I. Ashwood, et al., Phys. Rev. C 70 (2004) 024608.
[31] J. Simpson, et al., Acta Phys. Hung., New Series, Heavy Ion Phys. 11 (2000) 159.
[32] ENSDF, https://www.Go.bnl.gov/ensdf/.
[33] B. Le Crom, et al., Phys. Lett. B 829 (2022) 137057.
[34] X. Pereira-López, Study of transfer reactions induced by a ^{16}C beam, PhD Thesis, 2016, http://hal.in2p3.fr/tel-01522695.
[35] A. Matta, P. Morfouace, N. de Séréville, F. Flavigny, M. Labiche, R. Shearman, J. Phys. G 43 (2016) 045113.
[36] I.J. Thompson, Comput. Phys. Rep. 7 (1988) 167, http://www.fresco.org.uk/.
[37] Haixia An, Chonghai Cai, Phys. Rev. C 73 (2006) 054605.
[38] D.Y. Pang, et al., Phys. Rev. C 79 (2009) 024615.
[39] I. Brida, S.C. Pieper, R.B. Wiringa, Phys. Rev. C 84 (2011) 024319.
[40] W.W. Daehnick, J.D. Childs, Z. Vrcelj, Phys. Rev. C 21 (1980) 2253.
[41] J. Bojowald, et al., Phys. Rev. C 38 (1988) 1153.
[42] Y. Han, Y. Shi, Q. Shen, Phys. Rev. C 74 (2006) 044615.
[43] X. Li, Ch. Liang, Ch. Cai, Nucl. Phys. A 789 (2007) 103.
[44] G. Mairle, G.J. Wagner, Nucl. Phys. A 253 (1975) 253.
[45] M. Yasue, Nucl. Phys. A 509 (1990) 141.
[46] M.H. Macfarlane, J.B. French, Rev. Mod. Phys. 32 (1960) 567.
[47] D. Baye, N. Timofeyuk, Phys. Lett. B 293 (1992) 13.
[48] N. Timofeyuk, et al., Phys. Rev. C 86 (2012) 034305.
[49] B. Fernández-Domínguez, et al., Phys. Rev. C 91 (2015) 024307.
[50] V. Somà, T. Duguet, C. Barbieri, Phys. Rev. C 84 (2011) 064317.
[51] V. Somà, C. Barbieri, T. Duguet, Phys. Rev. C 89 (2014) 024323.
[52] V. Lapoux, et al., Phys. Rev. Lett. 117 (2016) 052501.
[53] V. Somà, C. Barbieri, T. Duguet, P. Navrátil, Eur. Phys. J. A 57 (2021) 135.
[54] G. Mairle, et al., Nucl. Phys. A 280 (1977) 97.
[55] M. Stanoiu, et al., Phys. Rev. C 78 (2008) 034315.
[56] C. Barbieri, T. Duguet, V. Somà, Phys. Rev. C 105 (2022) 044330.